Contributions of Climate Change, CO2 , Land-Use Change, and Human Activities to Changes in River Flow across 10 Chinese Basins

Yi Xi, Shushi Peng, Philippe Ciais, Matthieu Guimberteau, Yue Li, Shilong Piao, Xuhui Wang, Jan Polcher, Jiashuo Yu, Xuanze Zhang, et al.

Contributions of Climate Change, CO_2, Land-Use Change, and Human Activities to Changes in River Flow across 10 Chinese Basins

YI XI,[a] SHUSHI PENG,[a] PHILIPPE CIAIS,[a,b] MATTHIEU GUIMBERTEAU,[b,c] YUE LI,[a] SHILONG PIAO,[a] XUHUI WANG,[a,b] JAN POLCHER,[d] JIASHUO YU,[a] XUANZE ZHANG,[a] FENG ZHOU,[a] YAN BO,[a] CATHERINE OTTLE,[b] AND ZUN YIN[b]

[a] *Sino-French Institute for Earth System Science, College of Urban and Environmental Sciences, Peking University, Beijing, China*
[b] *Laboratoire des Sciences du Climat et de l'Environnement, LSCE/IPSL, CEA-CNRS-UVSQ, Université Paris-Saclay, Gif-sur-Yvette, France*
[c] *UMR 7619 METIS, Sorbonne Universités, UPMC, CNRS, EPHE, Paris, France*
[d] *Laboratoire de Météorologie Dynamique, CNRS, Palaiseau, France*

(Manuscript received 16 January 2018, in final form 3 October 2018)

ABSTRACT

As an essential source of freshwater river flow comprises ~80% of the water consumed in China. Per capita water resources in China are only a quarter of the global average, and its economy is demanding in water resources; this creates an urgent need to quantify the factors that contribute to changes in river flow. Here, we used an offline process-based land surface model (ORCHIDEE) at high spatial resolution (0.1° × 0.1°) to simulate the contributions of climate change, rising atmospheric CO_2 concentration, and land-use change to the change in natural river flow for 10 Chinese basins from 1979 to 2015. We found that climate change, especially an increase in precipitation, was responsible for more than 90% of the changes in natural river flow, while the direct effect of rising CO_2 concentration and land-use change contributes at most 6.3%. Nevertheless, rising CO_2 concentration and land-use change cannot be neglected in most basins as these two factors significantly change transpiration. From 2003 to 2015, the increase in water consumption offset more than 30% of the increase in natural river flow in northern China, especially in the Yellow River basin (~140%), but it had little effect on observed river flow in southern China. Although the uncertainties of rainfall data and the statistical water consumption data could propagate the uncertainties in simulated river flow, this study could be helpful for water planning and management in China under the context of global warming.

1. Introduction

Over the past five decades, significant warming and changes in the frequency and intensity of precipitation have been observed in China (Ding et al. 2007; Piao et al. 2010). These changes impact the whole hydrological cycle. Water use has also increased by 10% during the last two decades with the rapid growth in China's GDP of 6%–18% yr^{-1} [China Water Resources Bulletin 1997–2016 (Ministry of Water Resources 2018a); China Statistical Yearbook 1997–2016 (National Bureau of Statistics of China 2018)]. Currently, per capita water resources in China are only a quarter of the global average (Ge et al. 2011). Further, water resources in China have a highly uneven spatial distribution, with water deficits in northern China and flooding from high summer rainfall common in southern China (Ge et al. 2011; Piao et al. 2010). Both environmental changes and increased water consumption put stress on the available water resources (Alcamo et al. 2007; Vörösmarty et al. 2000; Xiong et al. 2010). Meeting the demand for water for agricultural, domestic, and industrial purposes from limited water resources is likely to be a challenge for the future. In China, river flow makes up ~80% of water consumption and is thus the main water source for human society. Especially in the context of climate change, this creates an urgent need to quantify and understand the factors that contribute to changes in river flow and allow water planning and management of China to be underpinned by sound scientific analysis.

Previous studies have detected a variety of trends in annual river flow among different basins in China

Supplemental information related to this paper is available at the Journals Online website: https://doi.org/10.1175/JHM-D-18-0005.s1.

Corresponding author: Shushi Peng, speng@pku.edu.cn

DOI: 10.1175/JHM-D-18-0005.1

(Fu et al. 2004; Wang et al. 2006; Xu et al. 2010; S. L. Yang et al. 2015; Zhang et al. 2006). In northern China, most basins show a persistent decline in river flow over the last five decades, such as Yellow, Hai, Liao, and Songhua Rivers (Piao et al. 2010; Wang et al. 2013; Zhang et al. 2017; Z. Zhang et al. 2011). In contrast, in southern China, there has been a significant increase in river flow in the Pearl, Southeast, and Southwest River basins, but little change in river flow in the Yangtze River basin (Piao et al. 2010; Xu et al. 2010; Yang et al. 2009; Ye et al. 2013). Nonparametric Mann–Kendall trend analysis, Budyko framework, Soil and Water Assessment Tool (SWAT), or process-based models [e.g., Community Land Model version 4 (CLM4), Variable Infiltration Capacity (VIC), Organizing Carbon and Hydrology in Dynamic Ecosystems (ORCHIDEE)] have already been applied to attribute the changes in river flow for a single or several basins in China (Jiang et al. 2011; Lei et al. 2014; Wang et al. 2013; H. Yang et al. 2015; S. L. Yang et al. 2015; Yin et al. 2017; Zhang et al. 2017; Z. Zhang et al. 2011). As shown in these studies, during different periods, the main factors influencing the river flow are different for different basins. For example, in the Laohahe and Hai River catchments and the Jinghe River basin, human activities accounted for the majority of runoff reduction over the last three decades (Jiang et al. 2011; Wang et al. 2013; Yin et al. 2017), while in Yangtze River, 60%–70% of the decline of mean water discharge from 2003 to 2012 could be attributed to decreased precipitation (S. L. Yang et al. 2015). Besides climate change and human activities, much attention has been paid to the effects of CO_2 concentration and land-use and land-cover changes on river flow (Piao et al. 2007; Yin et al. 2017), in the context of rising atmosphere CO_2 concentration and intensified land-use and land-cover change during the past century (Klein Goldewijk et al. 2011). However, there are few studies that comprehensively analyzed the impacts of climate change, rising CO_2 concentration, land-use change, and human activities on river flow at basin scale for China. The quantitative contributions of these four factors on river flow are still unclear, which urgently needs to be addressed.

The main purpose of this study is to evaluate the contributions of environmental factors (climate change, atmospheric CO_2 concentration, and land-use change) and water consumption by human activities to changes in annual river flow of large basins in China during the period 1979–2015. We used the land surface model ORCHIDEE (Krinner et al. 2005) to simulate the full hydrological cycle but without human water consumption/management; we term the output "natural river flow." Reconstructed natural river flows for each basin were calculated as the sum of observed river flow measured at the outlet gauging station and water consumption from water-use statistics. Simulated natural river flow by the ORCHIDEE model was confronted with this observation-based natural river flow. The contributions of climate change, atmospheric CO_2 concentration, and land-use change on the changes in natural river flow were then evaluated using factorial simulations with ORCHIDEE. Finally, we discussed the effect of water consumption on observed river flow and changes in the main hydrological processes such as evapotranspiration related to climate change, rising atmospheric CO_2 concentration, and land-use change.

2. Materials and methods

a. Observation-based natural river flow

At large-basin scale, observed annual river flows at the outlet gauging stations from 2003 to 2015 were obtained from the statistics of the River Sediment Bulletin of China (2003–15; Ministry of Water Resources 2018b). Annual water consumption data for seven out of the 10 basins were collected from the water resources bulletin of each basin (2003–15; Table 1). According to the technical outline of China's Water Resources Bulletin compiled by the Ministry of Water Resources (2018a), the water consumption is defined as the sum of water loss to the atmosphere, water loss in products, and domestic and livestock drinking water. That is, it is the sum of several main sectors: irrigation of farmland, forests and grasslands, industrial and domestic water, and water consumption for residents and livestock in rural areas. For each sector, water consumption is estimated as the difference of water withdrawal and return flow to surface water or groundwater. In these annual bulletins, mainland China is divided into 10 large river basins (RBs): Songhua RB, Liao RB, Hai RB, Yellow RB, Northwest RB, Huai RB, Yangtze RB, Southwest RB, Southeast RB, and Pearl RB. Figure 1 maps these 10 basins with their corresponding outlet gauging stations. The sum of observed annual river flow at an outlet gauging station and the annual water consumption in a basin is taken as the reconstructed natural river flow for that basin. Natural river flow in the Hai, Northwest, and Southwest RBs could not be reconstructed due to the unavailability of observed river flow and/or water consumption data from the annual bulletins. Thus, only seven basins were used for model evaluation. The detailed information about the outlet gauging stations with corresponding water consumption data for the seven basins can be found in Table 1. Note that we took only the main subbasin (Minjiang RB) into account for

TABLE 1. Outlet stations and water consumption data description of seven river basins in China. All datasets accessed September 2017.

Basin	Outlet station	Water consumption	
		Data source	Reference
Songhua	Jiamusi	Songliao RB Water Resources Bulletin (2003–15)	http://www.slwr.gov.cn/szy2011/
Liao	Liujianfang		
Yellow	Lijin	Yellow RB Water Resources Bulletin (2003–15)	http://www.yellowriver.gov.cn/other/hhgb/
Huai	Bengbu	Huai RB Water Resources Bulletin (2003–15)	http://www.hrc.gov.cn/main/szygb/index.jhtml
Yangtze	Datong	Yangtze RB Water Resources Bulletin (2003–15)	http://www.cjw.gov.cn/zwzc/bmgb/
Southeast	Zhuqi	Taihu basin and Southeast River Water Resource Bulletin (2003–15)	http://www.tba.gov.cn/channels/44.html
Pearl	Gaoyao, Shijiao, Boluo	Pearl River Water Resource Bulletin (2003–15)	http://www.pearlwater.gov.cn/xxcx/szygg/

Southeast RB, because only one outlet gauging station (Zhuqi) is reported in the River Sediment Bulletin.

b. ORCHIDEE model

ORCHIDEE (Trunk version r2916) is a process-based land surface model that simulates the fluxes and stores of water and carbon through the vegetation–soil–atmosphere system (Krinner et al. 2005). The model includes physical (SECHIBA) and carbon (STOMATE) modules which operate at 30-min and daily time steps, respectively. Based on prescribed land-cover maps including bare soil and 12 plant function types (PFTs; comprising nine forest types, C3 and C4 grasslands, and croplands), carbon and water budgets are simulated at the grid scale. An 11-layer soil hydrology scheme simulates vertical water flows based on a physical description of water diffusion and retention in unsaturated soils (Campoy et al. 2013; De Rosnay et al. 2000, 2002; Guimberteau et al. 2014). Accordingly, soil moisture is redistributed by solving the Richards equation for vertical unsaturated flow under the effect of root uptake and its controls on the evapotranspiration (ET), the sum of the transpiration, interception loss, bare soil evaporation, and snow sublimation. The precipitation rate and the soil hydraulic conductivity govern the partitioning between surface runoff and soil infiltration. A gravitational drainage is prescribed at the bottom of the soil column. The sum of surface runoff and drainage is transformed into river discharge by a river routing module (Guimberteau et al. 2012b), which calculates the daily continental runoff to the ocean.

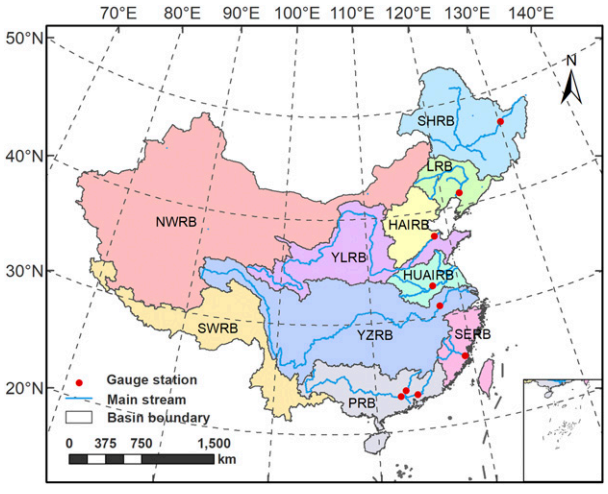

FIG. 1. Map of large river basins in China. The 10 river basins include Songhua River basin (SHRB), Liao River basin (LRB), Hai River basin (HAIRB), Yellow River basin (YLRB), Northwest River basin (NWRB), Huai River basin (HUAIRB), Yangtze River basin (YZRB), Southwest River basin (SWRB), Southeast River basin (SERB), and Pearl River basin (PRB). The outlet gauging stations are marked as red dots and listed in Table 1.

In the model, vegetation productivity is calculated based on a coupled photosynthesis–water balance scheme. Net plant carbon gain is mainly allocated to three tissue pools (leaf, root, and wood). Depending on soil temperature and moisture, the plant changes the relative investment into above- and below-ground structures (Friedlingstein et al. 1999). Thus, the ecosystem water balance influences plant carbon gains and structure. Leaf phenology and decomposition of litter and soil organic matter depend on temperature and water stress (Botta et al. 2000). The formulation of stomatal conductance is modeled following a semi-empirical approach (Yin et al. 2009), which ensures the consistency between the treatment of hydrological processes, especially transpiration, and the treatment of ecological processes. More detailed descriptions of the treatment of these processes can be found in Krinner et al. (2005) and Ducoudré et al. (1993).

The ORCHIDEE model has been widely used to estimate the transient impacts of climate change on the global or regional hydrological and carbon cycles (Guimberteau et al. 2013, 2017; Piao et al. 2006; Ringeval et al. 2012; Traore et al. 2014; Vérant et al. 2004; Zhu et al. 2015). The seasonal cycles of carbon and water fluxes in

ORCHIDEE were compared and validated with measurement data of eddy covariance sites (Krinner et al. 2005; Piao et al. 2013). The spatial distributions and temporal variations in LAI and runoff derived from satellite observations can be reproduced (Guimberteau et al. 2018; Krinner et al. 2005; Ringeval et al. 2012). The effects of rising CO_2 concentration on vegetation, including increasing the foliage area and partially closing stomata, were also evaluated at global and regional scale (Piao et al. 2007, 2013; Traore et al. 2014). The forcing datasets including climate data, soil and land-cover map, and simulation protocol are described below.

c. Forcing datasets

We forced ORCHIDEE with the China Meteorological Forcing Dataset (CMFD), which includes temperature, precipitation rate, pressure, specific humidity, wind speed, and downward shortwave and longwave radiation with a $0.1° \times 0.1°$ spatial resolution and 3-h temporal resolution from 1979 to 2015 (Chen et al. 2011). These climatic data assimilate meteorological observation data from the Chinese Meteorological Administration, Princeton reanalysis climate data, GLDAS reanalysis climate data, GEWEX-SRB radiation, and TRMM precipitation (He and Yang 2011). The historical changes in annual atmospheric CO_2 concentration were taken from the NOAA observations (Rayner et al. 2005). Land-cover maps were constructed by combining spatial information from the 1:1 000 000 Chinese vegetation map (Chinese Academy of Sciences 2001; Peng et al. 2011) and temporal variations in forest area at province level from the national forest inventory (Fang et al. 2014). First, the plant species in the Chinese vegetation map were grouped into 13 ORCHIDEE PFTs according to their climate regions, vegetation phenology type, and physiognomy based on the knowledge of flora of China (http://frps.eflora.cn/). Then, changes in every plant species of the vegetation maps established at province scale were evenly distributed into all the grid cells with the corresponding PFTs. The nonforest PFTs were adjusted proportionally to keep the area conserved. Because the forest inventory in China was taken every 5 years (i.e., the second National Forest Resource Inventory Report covers 1977–81), annual forest area from 1982 to 2011 was linearly interpolated. The land-cover maps of 1979–81 and 2012–15 were taken as those of years 1982 and 2011, respectively. More details about the algorithm are given in Li et al. (2018). Generally, in China, forest, cropland, and grassland are mainly distributed in the south and northeast, middle, and northwest, respectively (Fig. S1 in the online supplemental material). During the period 1979–2015, the total area of forest in China increased by 0.22 Mkm^2 (9.04%), while the area of grassland and cropland decreased by 0.08 (2.46%) and 0.15 Mkm^2 (6.96%), respectively. The soil map by USDA classification with 5′ resolution was from Reynolds et al. (2000).

TABLE 2. Simulation protocol in this study.

Simulation	Climate	CO_2	Land cover
S1	1979–2015	1979–2015	1979–2015
S2	1979–2015	1979–2015	1979
S3	1979–2015	1979	1979

d. Simulation protocol

To isolate the effects of climate change, atmospheric CO_2 concentration, and land-use change on natural river flow, three simulations were conducted with ORCHIDEE (see details in Table 2). In simulation S1, climate, atmospheric CO_2 concentration, and land-cover maps are all varied from 1979 to 2015. In simulation S2, only climate and atmospheric CO_2 concentration varied from 1979 to 2015, while land cover was held as in 1979. In simulation S3, only climate varied from 1979 to 2015, and both atmospheric CO_2 concentration and land cover were held at the level of 1979 (340 ppm). Thus, the difference between simulations S1 and S2 represents the effect of the land-use change on the hydrological cycle (evapotranspiration, runoff, etc.). The difference between S2 and S3 represents the effect of the atmospheric CO_2 concentration on the hydrological cycle. Given that the irrigation scheme was deactivated in our simulations because the irrigation module had not yet been fully tested with the new 11-layer hydrology scheme, and that neither industrial nor domestic water consumption were included in our simulations, river flow from simulation S1 is only comparable with reconstructed natural river flow rather than with observed river flow. The spinup took 150 years of simulation and was achieved by cycling the five years of climate forcing from 1979 to 1983 with constant preindustrial atmospheric CO_2 concentration (280 ppm), and a static land cover prescribed from year 1979. A 78-yr transient simulation from 1901 to 1978 after spinup was done with the cycled five years of climate forcing from 1979 to 1983, atmospheric CO_2 concentration from 1901 to 1978, and a static land cover prescribed from year of 1979.

e. Evaluation of model performance

To evaluate the accuracy of the simulated results, four metrics were computed for the simulated river flow by ORCHIDEE across the seven basins, including the root-mean-square error (RMSE), goodness of fit R^2, the ratio of RMSE to mean annual reconstructed river flow (RMSE/Mean), and index of agreement d [Eqs. (1)–(4)].

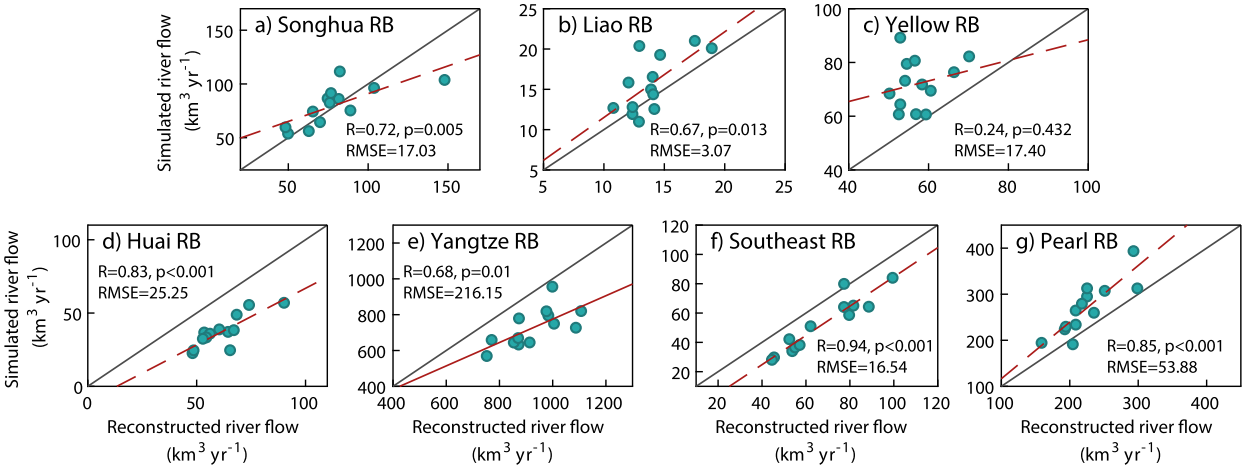

FIG. 2. (a)–(g) Comparison between annual simulated and reconstructed natural river flow for each basin during the period 2003–15. The solid and dashed lines are the 1:1 line and regression line, respectively.

These evaluation metrics estimate the error of the simulations and reflect how well the shape of the simulated natural river flow matches the shape of reconstructed river flow:

$$\mathrm{RMSE} = \sqrt{\frac{\sum_{i=1}^{n}(O_i - P_i)^2}{n}}, \tag{1}$$

$$\mathrm{RMSE/Mean} = \frac{\mathrm{RMSE}}{\overline{O}}, \tag{2}$$

$$R^2 = 1 - \frac{(O_i - P_i)^2}{(O_i - \overline{O})^2}, \quad \text{and} \tag{3}$$

$$d = 1 - \frac{\sum_{i=1}^{n}(O_i - P_i)^2}{\sum_{i=1}^{n}(|P_i - \overline{O}| - |O_i - \overline{O}|)^2}, \tag{4}$$

where O_i and P_i are the reconstructed and simulated annual natural river flow in the year i (from 2003 to 2015), respectively. Parameter $\overline{O}$ is the average of O_i from 2003 to 2015.

3. Results

a. *Comparison between simulated and reconstructed annual river flow*

Annual river flow outputs from ORCHIDEE are compared to reconstructed natural river flow (as described in section 2a) for each basin in Figs. 2 and 3. The simulated river flow agrees well with the reconstructed natural river flow in the Songhua and Liao RBs with high correlation coefficients (>0.67), but underestimates the reconstructed natural river flow in the Huai, Yangtze, and Southeast RBs, and overestimates in the Yellow and Pearl RBs. This can reflect model biases and natural river flow reconstruction biases. However, the ratio of RMSE between simulated and reconstructed natural river flow to the mean of reconstructed natural river flow is less than 25% in five out of the seven basins (Songhua, Liao, Yangtze, Southeast, and Pearl RBs; Table S1). The simulated river flow does follow the variations of reconstructed natural river flow in these basins, and the trends of simulated river flow do also follow the reconstructed natural river flow, even in the Yellow RB (Fig. 3), where the correlation coefficient and agreement index between simulated and reconstructed natural river flow is the lowest among seven basins (Table S1). This lower performance of ORCHIDEE in the Yellow RB (including most of the Loess Plateau) could result from missing processes in the model and/or from the reconstructed natural river flow. The latter could be subject to large errors because of uncertainties in water consumption, which makes the reconstructed natural river flow differ by up to 60% from the observed river flow (Fig. S2). Groundwater withdrawal, which is not accounted for, is also considerable in the Yellow RB.

b. *Spatial patterns of mean annual precipitation, evapotranspiration, and runoff*

Figure 4 shows the spatial patterns of mean annual precipitation P, simulated runoff Q, and evapotranspiration (ET), as well as the ratio of transpiration E_t to ET and the ratio of Q to P under simulation S1 for China from 1979 to 2015. ET comprises direct evaporation E_d, defined as the sum of evaporation from the soil, the evaporation of

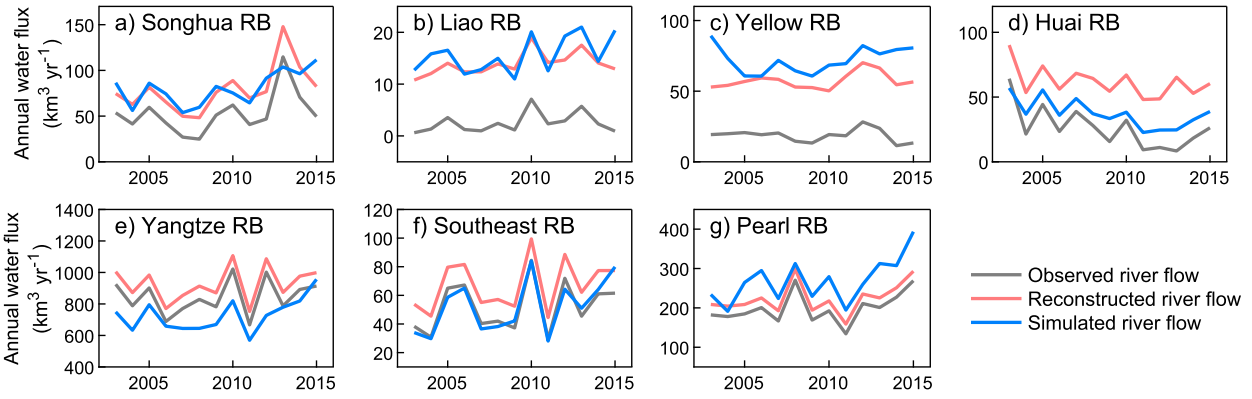

FIG. 3. (a)–(g) Temporal variations in annual observed river flow (gray line), natural river flow (red line), and river flow simulated by the ORCHIDEE model (blue line) in the seven basins of China from 2003 to 2015.

intercepted precipitation and snow sublimation, and E_t. Mean annual P decreases gradually from the southeast (more than 1000 mm yr^{-1}) to the inland northwest (less than 400 mm yr^{-1}). Mean annual E_t follows the spatial gradient of P (Fig. 4c). Direct evaporation E_d is higher than E_t across the upper reaches of the Yangtze and Southwest RBs and in small patches of the Songhua and Liao RBs and southeastern China (more than 500 mm yr^{-1}; Fig. 4b). In southern China, most of E_d is made up of interception loss, but bare soil evaporation contributes most of the evaporation in northern China (Fig. S3). Runoff generally follows the spatial gradient of P, with large areas of major runoff in the Southeast and Pearl RBs, and the lower reaches of the Yangtze RB (Fig. 4d). The spatial distribution of the ratio of E_t to ET shows that transpiration dominates ET in southern China while direct evaporation dominates ET in northern China (Fig. 4e). More than 50% of the precipitation goes directly into runoff in southern China, but less than 20% of the precipitation goes into runoff in northern China (Figs. 4f and S4).

c. *Covariations of annual runoff, precipitation, direct evaporation, and transpiration at basin scale*

Figure 5 shows the interannual variations in P, E_d, E_t, and Q for each basin without human activities (simulation S1) from 1979 to 2015. The correlation coefficients between detrended Q and P are significant (R = 0.75–0.95, $p < 0.001$) and much higher than those between detrended Q and both E_d and E_t in all basins (Table S2). This suggests that precipitation is the dominant driver for the interannual variability of runoff. Annual precipitation also significantly and positively correlates with E_d in most basins except in the Yangtze and Southeast, while the correlation coefficient between annual E_d and potential evaporation (PET) is negative in most basins (except Northwest RB), indicating that interannual variability of E_d is mainly related to the water supply for soil moisture and interception in most basins. In dryland regions such as the Northwest RB, the interannual variability of P drives interannual variability of E_d and Q, as well as E_t (Fig. 5e).

d. *Attribution of trends in annual evaporation, transpiration, and runoff at basin scale*

Figure 6 shows the attribution of the trends in simulated annual E_d, E_t, and Q across the 10 basins to climate change (CLIM), atmospheric CO_2 concentration (CO_2), and land-use change (LUC). Annual precipitation has positive trends in all 10 basins with significant positive trends in the Southeast, Northwest, Southwest, Songhua, and Yellow RBs (Fig. 6a). This increasing trend of annual P and changes in other climatic variables (Table S3) causes the increasing trends in E_t (Fig. 6c) and runoff (Fig. 6d) in all basins except the Northwest RB. In the Northwest RB, ~70% of the increased P is lost by E_d, while in other basins, 80%–90% of increased P is lost by Q, and the other 10%–20% of increased P is lost by E_t.

The trends of annual E_d across the 10 basins are mainly driven by climate change (Fig. 6b). Annual E_d exhibits decreases in 9 out of the 10 basins in simulation S3, while there is a large increase by 2.3 mm yr^{-2} in the Northwest RB (Fig. 6b). The decreasing E_d in the nine basins results from both decreasing bare soil evaporation and decreasing interception loss, but the increasing E_d in the Northwest RB is mainly contributed by the increasing evaporation from bare soil. The annual PET decreases in the Songhua, Liao, Huai, and Southeast RBs, resulting from decreasing net radiation and/or decreasing wind speed and/or increasing air humidity (Table S3). The decreasing net radiation and/or decreasing wind speed can partly explain the decreasing E_d in these basins. The increasing E_d in the Northwest RB

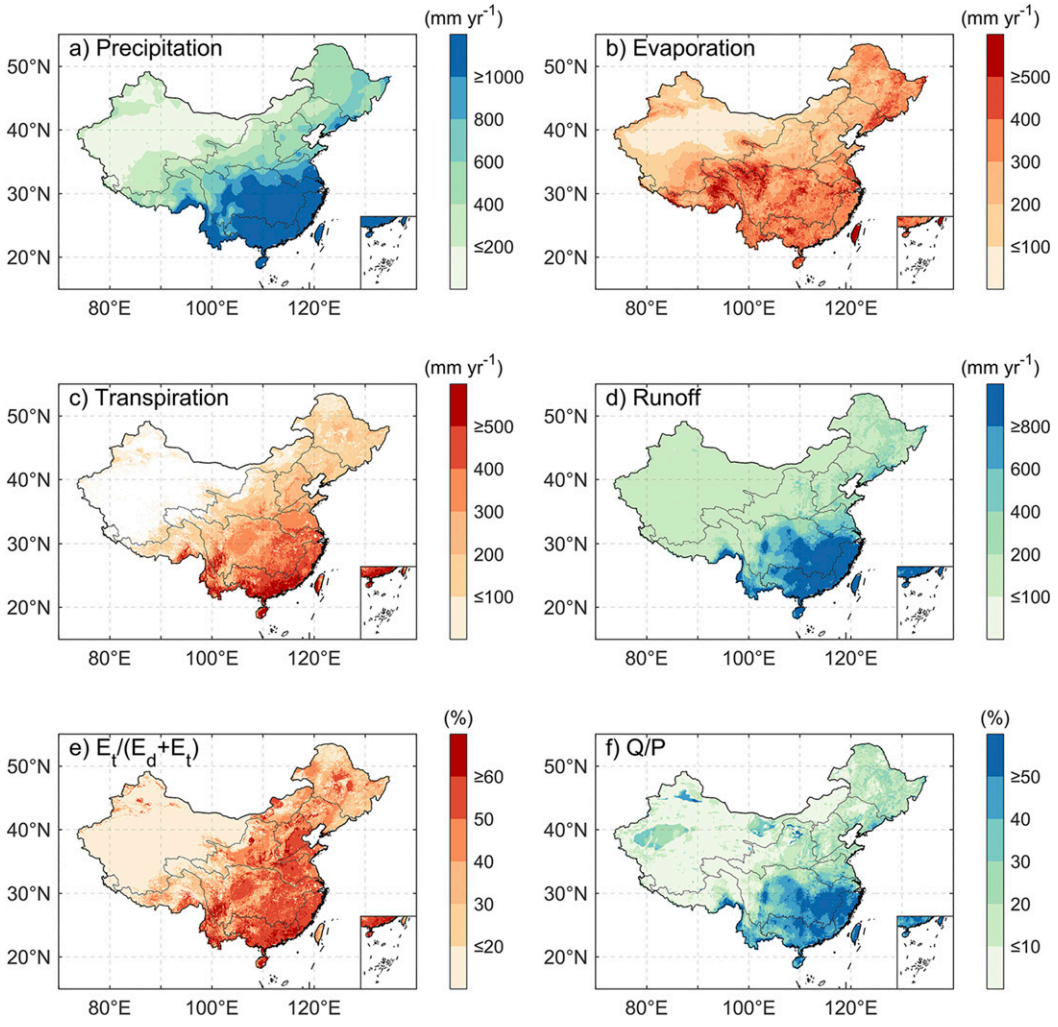

FIG. 4. Spatial patterns of mean annual (a) precipitation, (b) direct evaporation, (c) transpiration, (d) runoff, (e) ratio of transpiration E_t to evapotranspiration $E_d + E_t$, and (f) ratio of runoff Q to precipitation P in China from 1979 to 2015 under simulation S1 by ORCHIDEE.

can be attributed to greater evaporation from the soil due to increased soil water supply from increased precipitation (Fig. 6a), because the increase in PET (0.5 mm yr^{-2}; Table S3) is nonsignificant and small. LUC and the rising atmospheric CO_2 concentration have little effect on the trends of E_d.

Climate change contributes to significant positive trends in annual E_t in the Southeast (1.4 mm yr^{-2}), Southwest (0.8 mm yr^{-2}), and Northwest (0.2 mm yr^{-2}) RBs. The rising atmospheric CO_2 concentration decreases E_t across the 10 basins except for the Northwest RB, and significantly decreases E_t by ~0.3 mm yr^{-2} in the Southeast, Huai, and Pearl RBs. Annual E_t in the Pearl, Southwest, Songhua, Yangtze, and Southeast RBs significantly increased due to LUC. The contributions of LUC on trends of E_t reach 0.3–0.4 mm yr^{-2} in the Pearl and Southwest RBs. This could be related to the large area of afforestation and reforestation in these regions as discussed in section 4a.

Figure 6d and Table 3 summarize the contributions of the trends in simulated annual runoff across the 10 basins. Climate change resulted in significantly increased annual natural runoff (1–13 mm yr^{-2}) during the past 37 years, which contributes more than 90% to the trends of simulated runoff in all 10 basins. LUC and rising atmospheric CO_2 concentration have a very small influence on trends of annual runoff (<6.3%) compared with climate change.

Furthermore, we assessed the contribution of water consumption to the trends of reconstructed natural river flow in the seven basins with sufficient observation and statistics from 2003 to 2015. In Table 4, water

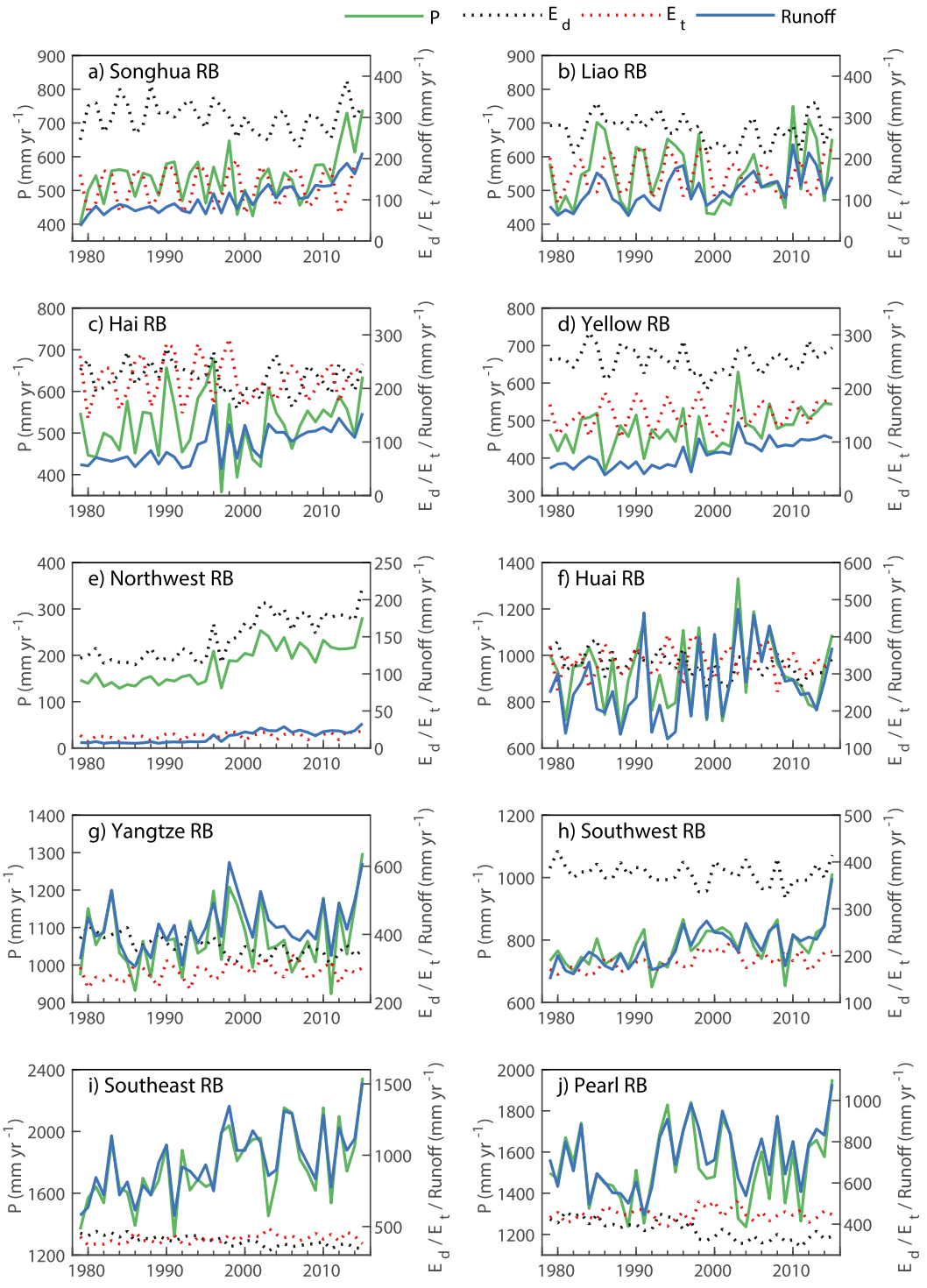

FIG. 5. (a)–(j) Temporal variation in annual P (displayed on the left axis) and E_d, E_t, and natural runoff (Runoff; displayed on the right axis) in the 10 basins of China from 1979 to 2015 under simulation S1 by ORCHIDEE.

consumption by human activities can offset more than 30% of the increase in annual natural river flow across the four basins in northern China, especially in the Yellow RB (~140%). Less than 10% of the trends of reconstructed natural river flow can be attributed to water consumption across the three basins in southern China because climate change has more influence on the variation in simulated natural river flow.

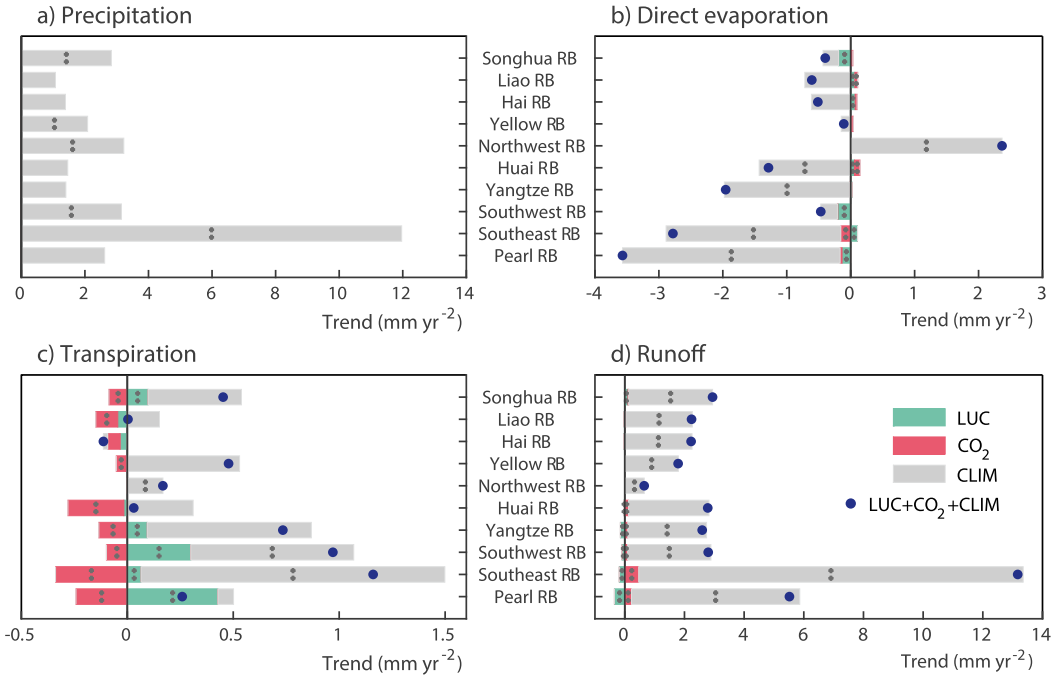

FIG. 6. Trend in (a) precipitation and attribution of trends in (b) direct evaporation, (c) transpiration, and (d) runoff in the 10 basins from 1979 to 2015 under simulation S1 by ORCHIDEE. The gray bars, red bars, green bars, and blue dots indicate trends driven by CLIM, rising CO_2, LUC, and all of them, respectively. Bars denoted by two asterisks indicate that the trends are statistically significant at the 95% ($p < 0.05$) level.

4. Discussion

a. *Contributions of climate change, rising atmospheric CO_2 concentration, and land-use change to the change in river flow*

The ORCHIDEE simulations isolate the impacts of climate change, rising atmospheric CO_2 concentration, and land-use change on annual natural river flow. Climate change, mainly changes in precipitation, drives the trends of annual natural river flow across the basins in China during the period 1979–2015. Besides precipitation, changes in short radiation, air temperature, air humidity, and wind speed could also contribute to changes in direct evaporation and transpiration (Table S3, Fig. S5). Furthermore, the attribution analysis for the variation in the transpiration and direct evaporation also suggests that the roles of CO_2 and land-use change should not be neglected in some basins.

TABLE 3. The relative contribution of CLIM, CO_2, and LUC to the trend of annual natural river flow for the 10 basins in Fig. 1 simulated by ORCHIDEE from 1979 to 2015. Note: the minus sign indicates the effect is negative.

Basin	LUC	CO_2	CLIM
Songhua	3.6%	0.9%	95.5%
Liao	−1.2%	1.5%	99.7%
Hai	−1.4%	0.0%	101.4%
Yellow	−0.5%	0.4%	100.1%
Northwest	0.0%	−0.1%	100.1%
Huai	−1.5%	4.6%	96.8%
Yangtze	−5.6%	3.8%	101.8%
Southwest	−3.3%	3.4%	99.8%
Southeast	−1.4%	3.6%	97.8%
Pearl	−6.3%	4.1%	102.2%

Over the last four decades, climate change is the main explanatory factor for the changes of direct evaporation, transpiration, and runoff in all basins, which accounts for more than 90% of the changes in simulated natural river flow in all basins. Interannual variability of natural runoff in all basins is driven by precipitation ($R = 0.75$–0.95; Fig. 6, Table S2). This is consistent with previous studies (Fu et al. 2004; Wang et al. 2013; Q. Zhang et al. 2011). For instance, in the Poyang Lake catchment (in the middle reaches of the Yangtze River), climate change resulted in an increased annual runoff of 75.3–261.7 mm from the 1970s to 2000s, accounting for 105.0%–212.1% of runoff changes relative to 1960s (Ye et al. 2013). In Pearl RB, the runoff has increased by 12% since the 1960s, owing to an increase in precipitation (Piao et al. 2010). However, a decrease in annual precipitation is detected in most basins over northern China such as the Songhuajiang, Liaohe, and Huai River basins during the period from the

TABLE 4. The trends of observed river flow, water consumption, reconstructed and simulated natural river flow, and the contribution of water consumption to the trend of natural river flow in the seven basins from 2003 to 2015. The bold italic values and the bold values show $p < 0.001$ and $p < 0.01$, respectively, and the italic values show $p < 0.05$. The contributions of water consumption to the trend of reconstructed natural river flow (the sixth column) are the ratios of water consumption (the third column) and the reconstructed natural river flow (the fourth column), and the contributions of water consumption to the trend of simulated natural river flow (the last column) are the ratios of water consumption (the third column) and the reconstructed natural river flow (the fifth column).

Basin	Trend from 2003 to 2015 ($km^3\ yr^{-2}$)				Contribution of water consumption to the trend of reconstructed natural river flow	Contribution of water consumption to the trend of simulated natural river flow
	Observed river flow	Water consumption	Reconstructed natural river flow	Simulated natural river flow		
Songhua	2.30	***1.16***	3.46	*2.81*	33.5%	41.3%
Liao	0.15	***0.14***	0.29	0.46	48.3%	30.4%
Yellow	−0.21	**0.74**	0.53	0.59	139.6%	125.4%
Huai	*-2.63*	*1.11*	−1.52	*−1.86*	−73.0%	−59.7%
Yangtze	5.07	*0.34*	5.41	12.82	6.3%	2.7%
Southeast	1.36	**0.14**	1.50	2.44	9.3%	5.7%
Pearl	3.95	−0.17	3.78	*8.42*	−4.5%	−2.0%

1950s to the 1980s/1990s, resulting in decrease in river flow (Liu and Du 2017). In the Jinghe River basin, climate change (decreased precipitation and increased temperature) contributed to 88% of the runoff decrease between 1970s and the 1980s (Yin et al. 2017). In Hai RB, impacts of climate variation were accountable for the runoff decrease by 26.9% during the past 50 years (1956–2005; Xu et al. 2014). In this study, the positive trends of natural river flow from 1979 to 2015 in both northern and southern China could be mainly ascribed to the recent decadal increased precipitation (Fig. 6). To evaluated the accuracy of the results, we compared the precipitation data used in this study (CMFD) with Multi-Source Weighted-Ensemble Precipitation (MSWEP; Beck et al. 2017), Climatic Research Unit (CRU), and ERA-Interim (Dee et al. 2011; see details in section S1 in the supplemental material). From 1979 to 2015, there are also increasing precipitation trends in at least one other dataset in four RBs (Yellow, Northwest, Southwest, and Southwest RBs) where significant positive trends are shown in CMFD. In other RBs, there are some divergences in the trend in annual precipitation among different datasets, but most of them are not significant. Limited by the number and spatial coverage of surface stations and/or different satellite retrieved algorithms and/or different data assimilation models used in different precipitation datasets, there are large discrepancies in both the magnitude and variability in precipitation estimates (Sun et al. 2018), which could definitely result in large uncertainty in simulated river flow. Besides precipitation, increased temperature and decreased wind speed and net radiation can also significantly influence river flow by changing ET (Table S3). The decrease in the interception loss also contributes to the decrease in E_d simulated by ORCHIDEE in southern China, but this needs further observational data to verify (Fig. S3).

The possible effects of rising atmospheric CO_2 concentration on river flow have been the subject of international debate for more than a decade (Gedney et al. 2006; Piao et al. 2007; Trancoso et al. 2017). On the one hand, elevated CO_2 can enhance LAI, and consequently evapotranspiration, which would result in reduced river flow (Cowling and Field 2003; Zhu et al. 2016). On the other hand, elevated CO_2 also reduces transpiration per unit leaf area because plants react by partially closing their stomata, a process which can increase river flow (Field et al. 1995). At continental scale, simulation of river runoff based on ORCHIDEE indicates that these two opposite effects of elevated CO_2 might offset each other (Piao et al. 2007). However, elevated CO_2 could have substantial and drastically different effects on river flow at local level. Shi et al. (2011) found that rising CO_2 accounts for an upward trend in river flow in the Amazon River and Yangtze RB from 1948 to 2004 ($0.0274\,km^3\,yr^{-2}$), while Ukkola et al. (2016) and Trancoso et al. (2017) found that rising CO_2 concentration leads to significant reductions in streamflow in semiarid Australian regions and eastern Australia over the last three decades. The regionally heterogeneous effects of CO_2 on river flow could be related to different responses of vegetation to elevated CO_2 (enhanced LAI versus stomata closure) in specific catchments.

In our simulation, rising atmospheric CO_2 concentration significantly increases annual mean LAI from 1979 to 2015 (difference in LAI between simulations S2 and S3; Fig. 7a), with larger positive trends of LAI in southern China ($0.004\,m^2\,m^{-2}\,yr^{-1}$). However, with ~60 ppm increase in atmospheric CO_2 concentration from 1979 to 2015, the sensitivity of transpiration rate to CO_2 is estimated to be from −0.4 to $-0.2\,mm\,ppm^{-1}$ across the 10 basins (Fig. 7b). This suggests that decrease in transpiration due to stomatal closure is larger than

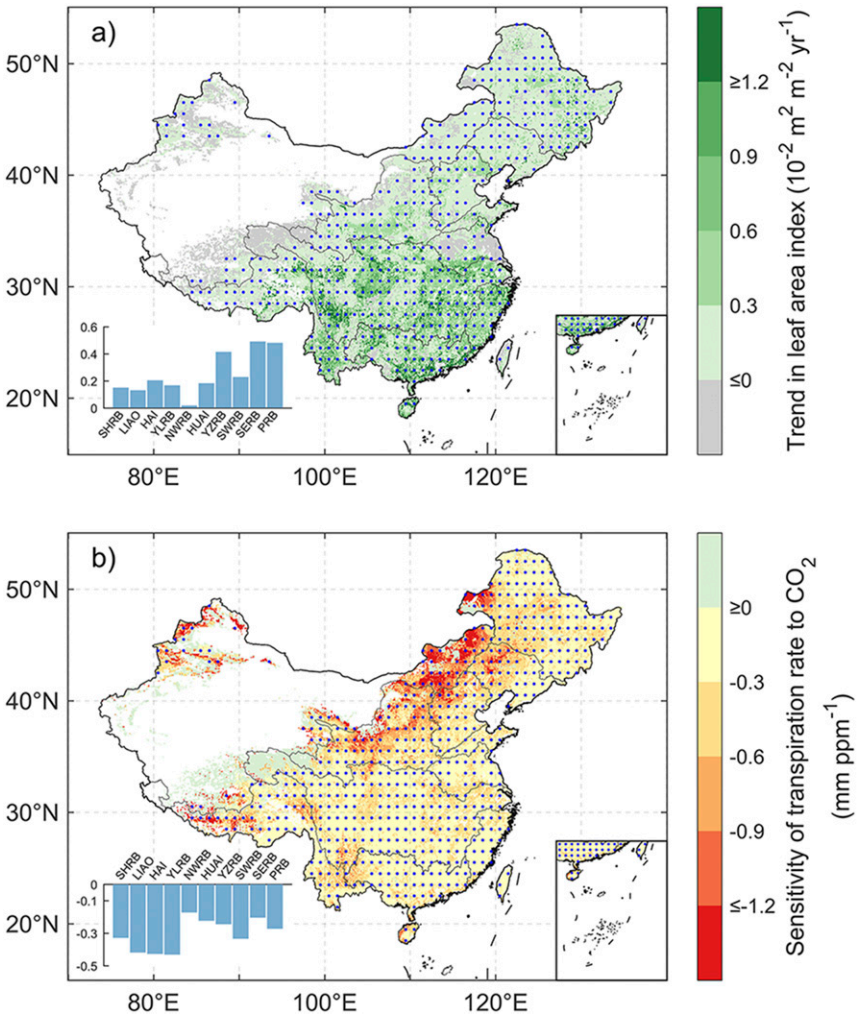

FIG. 7. Spatial patterns of the trends in (a) LAI and (b) sensitivity of transpiration per LAI (E_t/LAI) to atmospheric CO_2 concentration in China from 1979 to 2015 as simulated by ORCHIDEE. The blue dots indicate that the trends are statistically significant ($p < 0.05$). The two insets show the trends of LAI and sensitivity of the transpiration rate to atmospheric CO_2 concentration in the 10 basins of China from 1979 to 2015, respectively.

increase in transpiration due to increased LAI at basin scale. However, this decrease in transpiration caused by rising atmospheric CO_2 concentration is much smaller than the increased precipitation in most basins, so the contribution of rising atmospheric CO_2 concentration on the trend of runoff is masked by the change in precipitation across the 10 basins, which is consistent with the previous studies. In Hai RB, using another land surface model (CLM4), Lei et al. (2014) found that rising atmospheric CO_2 concentration only contributes 1.6% of the trend of annual runoff. Our analysis suggests the historically rising atmospheric CO_2 concentration during the last five decades had limited effect on runoff at the large basin scale, but the analysis does not allow us to look at the possible effect of the large increases in atmospheric CO_2 concentration specified under the future scenarios of the IPCC (IPCC 2013). The performance of the model to rising CO_2 concentration was evaluated in supplemental section S2.

Land-use change generally accounts for less than 6% of trends of natural runoff in China (Fig. 6d, Table 3), most notably in the Pearl, Yangtze, Southwest, and Songhua RBs. This could be related to the large area of afforestation and reforestation in the Pearl, Yangtze, and Southwest RBs (Fig. 8). The spatial distribution of the trend in forest area during the period 1982–2011 shows that southern China experienced the largest increase of forest area. This can explain the effects of LUC on transpiration across the 10 basins in Fig. 6c. Note that forest cover slightly decreases in Songhua RB because of

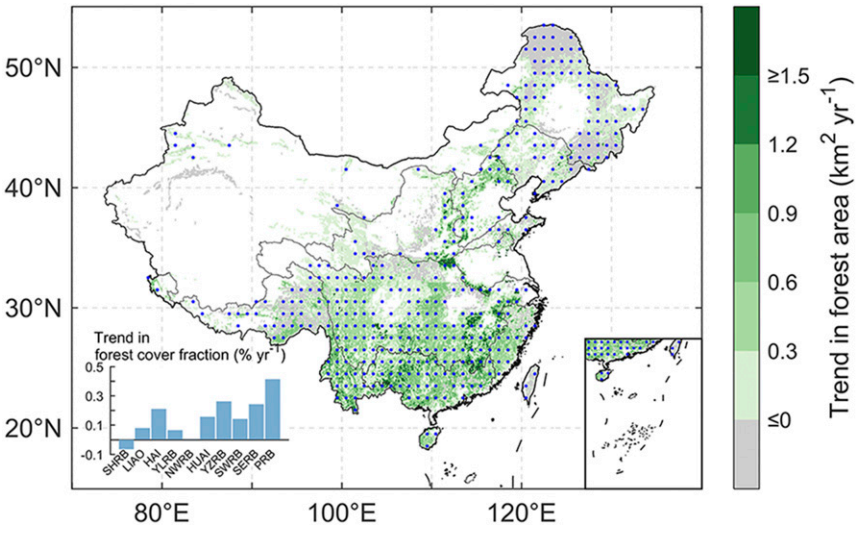

FIG. 8. Spatial pattern of the trend in forest area in China from 1982 to 2011. The blue dots indicate that the trends are statistically significant ($p < 0.05$). The inset shows the trends of forest cover fraction in the 10 basins of China from 1982 to 2011.

deforestation and cropland expansion in this region (Deng et al. 2010; Ye et al. 2009) during the last three decades, but LUC slightly increases simulated transpiration in the Songhua RB (Fig. 6c). This could be related to slightly increased LAI after the replacement of needleleaf forest with broadleaf forest and croplands, which has larger or similar LAI than needleleaf forest in the Songhua RB. The effects of LUC on runoff depend on climate and catchment characteristics (Zhou et al. 2015). Based on ground measurements and remotely sensed vegetation growth and evapotranspiration, Feng et al. (2016) show that 100% revegetation under the "Grain to Green" program can decrease runoff by about 20%–40% in catchments over the Loess Plateau during the 2000s. In southern China, however, forest recovery has little effect on river discharge during the past 50 years in Guangdong Province, where the forest area almost doubled (Zhou et al. 2010). Currently, China has the largest planted forest area in the world, and it is set to keep on increasing in the coming decades (FAO 2010; Peng et al. 2014). How and where afforestation and reforestation will impact river flow is still an open question (Cao 2011; Chen et al. 2015). This question calls for more observational data and paired catchment experiments and modeling studies in the future.

In addition, nitrogen deposition exceeds 20 kg N $ha^{-1} yr^{-1}$ and fertilizer addition in croplands reaches 200 kg N $ha^{-1} yr^{-1}$ in southern China (China Statistical Yearbook 2003–15; National Bureau of Statistics of China 2018; Liu et al. 2013). Nitrogen deposition and fertilizer addition as part of cropland management are not included in the ORCHIDEE model used in this study. Thus, our simulation S1 may have underestimated the increasing trends of LAI as well as trends of transpiration in forests, grasslands, and croplands in southern China (see detailed evaluation in supplemental section S3). This underestimation of the trend in transpiration could explain the overestimated trends of natural river flow in simulation S1 when compared with the reconstructed natural river flow in these three southern basins of China (Table 4). Since satellite LAI products have large uncertainty for mean, trends, and variability (Jiang et al. 2017), long-term ground-based LAI observations are needed for further model validation.

b. *Contribution of water consumption and management by humans*

The water consumption significantly increased by 0.1–1.2 $km^3 yr^{-2}$ from 2003 to 2015 across the six basins, except for the Pearl RB (Table 4). The increase in water consumption by human activities results in decreases in observed river flow in these RBs. In the Yellow RB, although natural river flow increased by 0.5 $km^3 yr^{-2}$, observed river flow still decreased by 0.2 $km^3 yr^{-2}$ because of the increase in water consumption by 0.7 $km^3 yr^{-2}$. In northern basins of China, increased water consumption significantly contributes to reconstructed river flow, but it contributes little to reconstructed river flow in southern basins of China (Table 4). This difference is closely related to the fraction of water consumption in natural river flow (Fig. S2). In previous studies, water consumption has been confirmed to dominate the decrease of river flow in most catchments in northern China (Fu et al. 2004; Jiang et al. 2011; Wang et al. 2009),

as well as for basins in eastern China (Zhang et al. 2014). The decline in annual river flow from the Yellow RB due to human activities ranged from 59% to 77% during the period 1993–2007 (Guo et al. 2014). Water consumption in Jingjinji Metropolitan Region (Beijing–Tianjin–Hebei) results in a 50% runoff reduction in the Hai RB from 1957 to 2000 (Wang et al. 2013). Water demand keeps increasing, and the pressure of water consumption on river flow could be enhanced. Besides the effects of water consumptions on river flow, water management such as transbasin diversion of water can significantly impact river flow (H. Yang et al. 2015). However, neither water consumption nor management are commonly represented in processed-based land surface models, although irrigation may be. It is important to include water consumption such as irrigation and dams/reservoirs in Earth system models to predict future water resources, as irrigation could have climate feedbacks and consequent impacts on river flow (Guimberteau et al. 2012a; Müller Schmied et al. 2016). In addition, any uncertainty of the statistical water consumption data will contribute to the uncertainty in reconstructed natural river flow, especially in some northern basins, where water consumption contributes 35%–80% to reconstructed natural river flow (Fig. S2).

5. Conclusions

In this study, we quantified the contributions of climate change, rising atmospheric CO_2 concentration, and land-use change on natural river flow in 10 Chinese basins by model simulations from 1979 to 2015. During this period, climate change can explain most of the increased natural river flow (more than 90%) across these 10 basins, of which precipitation is the main factor driving the interannual variability of natural river flow. Rising atmospheric CO_2 concentration can slightly (less than 5%) increase natural river flow, and land-use change (mainly by afforestation and reforestation) can slightly (less than 6%) decrease natural river flow across the basins in China. For the observed river flows, climate change controls their changes across the basins in southern China, while water consumption controls those in northern China from 2003 to 2015. However, the accuracy of observed river flow and water consumption data still needs to be quantified. Besides water consumption, water management such as transbasin diversion of water also impacts river flow, but this is not represented either in models or in statistics. Parameterization of nitrogen deposition, nitrogen fertilizer in croplands and cropland management, groundwater exchange, and dams are all ongoing developments of ORCHIDEE. For future water planning and management under the context of global warming, it is necessary to incorporate these natural and human-activity processes into the processed-based land surface models that are used in Earth system modeling.

Acknowledgments. This study was supported by the National Natural Science Foundation of China (Grants 41561134016, 41671079), the National Key Research and Development Program of China (2016YFC0500203), and by the CHINA-TREND-STREAM French national project (ANR Grant ANR-15-CE01-00L1-0L). Philippe Ciais and Matthieu Guimberteau were supported by the European Research Council Synergy Grant ERC-2013-SyG-610028 IMBALANCE-P.

REFERENCES

Alcamo, J., M. Flörke, and M. Märker, 2007: Future long-term changes in global water resources driven by socio-economic and climatic changes. *Hydrol. Sci. J.*, **52**, 247–275, https://doi.org/10.1623/hysj.52.2.247.

Beck, H. E., A. I. J. M. van Dijk, V. Levizzani, J. Schellekens, D. G. Miralles, B. Martens, and A. de Roo, 2017: MSWEP: 3-hourly 0.25 global gridded precipitation (1979–2015) by merging gauge, satellite, and reanalysis data. *Hydrol. Earth Syst. Sci.*, **21**, 589–615, https://doi.org/10.5194/hess-21-589-2017.

Botta, A., N. Viovy, P. Ciais, P. Friedlingstein, and P. Monfray, 2000: A global prognostic scheme of leaf onset using satellite data. *Global Change Biol.*, **6**, 709–725, https://doi.org/10.1046/j.1365-2486.2000.00362.x.

Campoy, A., A. Ducharne, F. Cheruy, F. Hourdin, J. Polcher, and J. Dupont, 2013: Response of land surface fluxes and precipitation to different soil bottom hydrological conditions in a general circulation model. *J. Geophys. Res. Atmos.*, **118**, 10 725–10 739, https://doi.org/10.1002/jgrd.50627.

Cao, S., 2011: Impact of China's large-scale ecological restoration program on the environment and society in arid and semiarid areas of China: Achievements, problems, synthesis, and applications. *Crit. Rev. Environ. Sci. Technol.*, **41**, 317–335, https://doi.org/10.1080/10643380902800034.

Chen, Y., K. Yang, J. He, J. Qin, J. Shi, J. Du, and Q. He, 2011: Improving land surface temperature modeling for dry land of China. *J. Geophys. Res.*, **116**, D20104, https://doi.org/10.1029/2011JD015921.

——, K. Wang, Y. Lin, W. Shi, Y. Song, and X. He, 2015: Balancing green and grain trade. *Nat. Geosci.*, **8**, 739–741, https://doi.org/10.1038/ngeo2544.

Chinese Academy of Sciences, 2001: *Vegetation Atlas of China* (in Chinese). Science Press, 260 pp.

Cowling, S. A., and C. B. Field, 2003: Environmental control of leaf area production: Implications for vegetation and land-surface modeling. *Global Biogeochem. Cycles*, **17**, 1007, https://doi.org/10.1029/2002GB001915.

Dee, D., and Coauthors, 2011: The ERA-Interim reanalysis: Configuration and performance of the data assimilation system. *Quart. J. Roy. Meteor. Soc.*, **137**, 553–597, https://doi.org/10.1002/qj.828.

Deng, X., Q. O. Jiang, H. Su, and F. Wu, 2010: Trace forest conversions in Northeast China with a 1-km area percentage data model. *J. Appl. Remote Sens.*, **4**, 041893, https://doi.org/10.1117/1.3491193.

De Rosnay, P., M. Bruen, and J. Polcher, 2000: Sensitivity of surface fluxes to the number of layers in the soil model used in GCMs. *Geophys. Res. Lett.*, **27**, 3329–3332, https://doi.org/10.1029/2000GL011574.

——, J. Polcher, M. Bruen, and K. Laval, 2002: Impact of a physically based soil water flow and soil-plant interaction representation for modeling large-scale land surface processes. *J. Geophys. Res.*, **107**, 4118, https://doi.org/10.1029/2001JD000634.

Ding, Y., and Coauthors, 2007: China's national assessment report on climate change (I): climate change in China and the future trend. *Adv. Climate Change Res.*, **3** (Suppl.), 1–5.

Ducoudré, N. I., K. Laval, and A. Perrier, 1993: SECHIBA, a new set of parameterizations of the hydrologic exchanges at the land-atmosphere interface within the LMD atmospheric general circulation model. *J. Climate*, **6**, 248–273, https://doi.org/10.1175/1520-0442(1993)006<0248:SANSOP>2.0.CO;2.

Fang, J., Z. Guo, H. Hu, T. Kato, H. Muraoka, and Y. Son, 2014: Forest biomass carbon sinks in East Asia, with special reference to the relative contributions of forest expansion and forest growth. *Global Change Biol.*, **20**, 2019–2030, https://doi.org/10.1111/gcb.12512.

FAO, 2010: Global Forest Resources Assessment 2010. Accessed 31 May 2017, http://www.fao.org/forestry/fra/fra2010/en/.

Feng, X., and Coauthors, 2016: Revegetation in China's Loess Plateau is approaching sustainable water resource limits. *Nat. Climate Change*, **6**, 1019–1022, https://doi.org/10.1038/nclimate3092.

Field, C. B., R. B. Jackson, and H. A. Mooney, 1995: Stomatal responses to increased CO_2: Implications from the plant to the global scale. *Plant Cell Environ.*, **18**, 1214–1225, https://doi.org/10.1111/j.1365-3040.1995.tb00630.x.

Friedlingstein, P., G. Joel, C. B. Field, and I. Y. Fung, 1999: Toward an allocation scheme for global terrestrial carbon models. *Global Change Biol.*, **5**, 755–770, https://doi.org/10.1046/j.1365-2486.1999.00269.x.

Fu, G., S. Chen, C. Liu, and D. Shepard, 2004: Hydro-climatic trends of the Yellow River Basin for the last 50 years. *Climatic Change*, **65**, 149–178, https://doi.org/10.1023/B:CLIM.0000037491.95395.bb.

Ge, L., G. Xie, C. Zhang, S. Li, Y. Qi, S. Cao, and T. He, 2011: An evaluation of China's water footprint. *Water Resour. Manage.*, **25**, 2633–2647, https://doi.org/10.1007/s11269-011-9830-1.

Gedney, N., P. M. Cox, R. A. Betts, O. Boucher, C. Huntingford, and P. A. Stott, 2006: Detection of a direct carbon dioxide effect in continental river runoff records. *Nature*, **439**, 835–838, https://doi.org/10.1038/nature04504.

Guimberteau, M., K. Laval, A. Perrier, and J. Polcher, 2012a: Global effect of irrigation and its impact on the onset of the Indian summer monsoon. *Climate Dyn.*, **39**, 1329–1348, https://doi.org/10.1007/s00382-011-1252-5.

——, and Coauthors, 2012b: Discharge simulation in the sub-basins of the Amazon using ORCHIDEE forced by new datasets. *Hydrol. Earth Syst. Sci.*, **16**, 911–935, https://doi.org/10.5194/hess-16-911-2012.

——, and Coauthors, 2013: Future changes in precipitation and impacts on extreme streamflow over Amazonian sub-basins. *Environ. Res. Lett.*, **8**, 014035, https://doi.org/10.1088/1748-9326/8/1/014035.

——, A. Ducharne, P. Ciais, J.-P. Boisier, S. Peng, M. De Weirdt, and H. Verbeeck, 2014: Testing conceptual and physically based soil hydrology schemes against observations for the Amazon Basin. *Geosci. Model Dev.*, **7**, 1115–1136, https://doi.org/10.5194/gmd-7-1115-2014.

——, and Coauthors, 2017: Impacts of future deforestation and climate change on the hydrology of the Amazon Basin: A multi-model analysis with a new set of land-cover change scenarios. *Hydrol. Earth Syst. Sci.*, **21**, 1455–1475, https://doi.org/10.5194/hess-21-1455-2017.

——, and Coauthors, 2018: ORCHIDEE-MICT (v8.4.1), a land surface model for the high latitudes: Model description and validation. *Geosci. Model Dev.*, **11**, 121–163, https://doi.org/10.5194/gmd-11-121-2018.

Guo, Y., Z. Li, M. Amo-Boateng, P. Deng, and P. Huang, 2014: Quantitative assessment of the impact of climate variability and human activities on runoff changes for the upper reaches of Weihe River. *Stochastic Environ. Res. Risk. Assess.*, **28**, 333–346, https://doi.org/10.1007/s00477-013-0752-8.

He, J., and K. Yang, 2011: China Meteorological Forcing Dataset. Cold and Arid Regions Science Data Center at Lanzhou, accessed 1 January 2017, https://doi.org/10.3972/westdc.002.2014.db.

IPCC, 2013: *Climate Change 2013: The Physical Science Basis*. Cambridge University Press, 1535 pp., https://doi.org/10.1017/CBO9781107415324.

Jiang, C., Y. Ryu, H. Fang, R. Myneni, M. Claverie, and Z. Zhu, 2017: Inconsistencies of interannual variability and trends in long-term satellite leaf area index products. *Global Change Biol.*, **23**, 4133–4146, https://doi.org/10.1111/gcb.13787.

Jiang, S., L. Ren, B. Yong, V. P. Singh, X. Yang, and F. Yuan, 2011: Quantifying the effects of climate variability and human activities on runoff from the Laohahe basin in northern China using three different methods. *Hydrol. Processes*, **25**, 2492–2505, https://doi.org/10.1002/hyp.8002.

Klein Goldewijk, K., A. Beusen, G. van Drecht, and M. de Vos, 2011: The HYDE 3.1 spatially explicit database of human-induced global land-use change over the past 12,000 years. *Global Ecol. Biogeogr.*, **20**, 73–86, https://doi.org/10.1111/j.1466-8238.2010.00587.x.

Krinner, G., and Coauthors, 2005: A dynamic global vegetation model for studies of the coupled atmosphere-biosphere system. *Global Biogeochem. Cycles*, **19**, GB1015, https://doi.org/10.1029/2003GB002199.

Lei, H., D. Yang, and M. Huang, 2014: Impacts of climate change and vegetation dynamics on runoff in the mountainous region of the Haihe River basin in the past five decades. *J. Hydrol.*, **511**, 786–799, https://doi.org/10.1016/j.jhydrol.2014.02.029.

Li, Y., and Coauthors, 2018: Divergent hydrological response to large-scale afforestation and vegetation greening in China. *Sci. Adv.*, **4**, eaar418, https://doi.org/10.1126/sciadv.aar4182.

Liu, L. L., and J. J. Du, 2017: Documented changes in annual runoff and attribution since the 1950s within selected rivers in China. *Adv. Climate Change Res.*, **8**, 37–47, https://doi.org/10.1016/j.accre.2017.03.005.

Liu, X., and Coauthors, 2013: Enhanced nitrogen deposition over China. *Nature*, **494**, 459–462, https://doi.org/10.1038/nature11917.

Ministry of Water Resources, 2018a: Chinese Water Resources Bulletin. Ministry of Water Resources of the People's Republic of China, http://www.mwr.gov.cn/sj/tjgb/szygb/.

——, 2018b: Chinese River Sediment Bulletin. Ministry of Water Resources of the People's Republic of China, http://www.mwr.gov.cn/sj/tjgb/zghlnsgb/.

Müller Schmied, H., and Coauthors, 2016: Variations of global and continental water balance components as impacted by climate forcing uncertainty and human water use. *Hydrol. Earth Syst. Sci.*, **20**, 2877–2898, https://doi.org/10.5194/hess-20-2877-2016.

National Bureau of Statistics of China, 2018: China Statistical Yearbook. National Bureau of Statistics of China, http://www.stats.gov.cn/english/statisticaldata/annualdata/.

Peng, S., and Coauthors, 2011: Recent change of vegetation growth trend in China. *Environ. Res. Lett.*, **6**, 044027, https://doi.org/10.1088/1748-9326/6/4/044027.

——, and Coauthors, 2014: Afforestation in China cools local land surface temperature. *Proc. Natl. Acad. Sci. USA*, **111**, 2915–2919, https://doi.org/10.1073/pnas.1315126111.

Piao, S., P. Friedlingstein, P. Ciais, L. Zhou, and A. Chen, 2006: Effect of climate and CO_2 changes on the greening of the Northern Hemisphere over the past two decades. *Geophys. Res. Lett.*, **33**, L23402, https://doi.org/10.1029/2006GL028205.

——, ——, ——, N. de Noblet-Ducoudré, D. Labat, and S. Zaehle, 2007: Changes in climate and land use have a larger direct impact than rising CO_2 on global river runoff trends. *Proc. Natl. Acad. Sci. USA*, **104**, 15 242–15 247, https://doi.org/10.1073/pnas.0707213104.

——, and Coauthors, 2010: The impacts of climate change on water resources and agriculture in China. *Nature*, **467**, 43–51, https://doi.org/10.1038/nature09364.

——, and Coauthors, 2013: Evaluation of terrestrial carbon cycle models for their response to climate variability and to CO_2 trends. *Global Change Biol.*, **19**, 2117–2132, https://doi.org/10.1111/gcb.12187.

Rayner, P. J., M. Scholze, W. Knorr, T. Kaminski, R. Giering, and H. Widmann, 2005: Two decades of terrestrial carbon fluxes from a carbon cycle data assimilation system (CCDAS). *Global Biogeochem. Cycles*, **19**, GB2026, https://doi.org/10.1029/2004GB002254.

Reynolds, C. A., T. J. Jackson, and W. J. Rawls, 2000: Estimating soil water-holding capacities by linking the Food and Agriculture Organization Soil map of the world with global pedon databases and continuous pedotransfer functions. *Water Resour. Res.*, **36**, 3653–3662, https://doi.org/10.1029/2000WR900130.

Ringeval, B., and Coauthors, 2012: Modelling sub-grid wetland in the ORCHIDEE global land surface model: Evaluation against river discharges and remotely sensed data. *Geosci. Model Dev.*, **5**, 941–962, https://doi.org/10.5194/gmd-5-941-2012.

Shi, X., J. Mao, P. E. Thornton, F. M. Hoffman, and W. M. Post, 2011: The impact of climate, CO2, nitrogen deposition and land use change on simulated contemporary global river flow. *Geophys. Res. Lett.*, **38**, L08704, https://doi.org/10.1029/2011GL046773.

Sun, Q., C. Miao, Q. Duan, H. Ashouri, S. Sorooshian, and K.-L. Hsu, 2018: A review of global precipitation data sets: Data sources, estimation, and intercomparisons. *Rev. Geophys.*, **56**, 79–107, https://doi.org/10.1002/2017RG000574.

Trancoso, R., J. R. Larsen, T. R. McVicar, S. R. Phinn, and C. A. McAlpine, 2017: CO_2-vegetation feedbacks and other climate changes implicated in reducing base flow. *Geophys. Res. Lett.*, **44**, 2310–2318, https://doi.org/10.1002/2017GL072759.

Traore, A. K., and Coauthors, 2014: Evaluation of the ORCHIDEE ecosystem model over Africa against 25 years of satellite-based water and carbon measurements. *J. Geophys. Res. Biogeosci.*, **119**, 1554–1575, https://doi.org/10.1002/2014JG002638.

Ukkola, A. M., I. C. Prentice, T. F. Keenan, A. I. J. M. van Dijk, N. R. Viney, and R. B. Myeni, and J. Bi, 2016: Reduced streamflow in water-stressed climates consistent with CO2 effects on vegetation. *Nat. Climate Change*, **6**, 75–78, https://doi.org/doi:10.1038/nclimate2831.

Vérant, S., K. Laval, J. Polcher, and M. D. Castro, 2004: Sensitivity of the continental hydrological cycle to the spatial resolution over the Iberian Peninsula. *J. Hydrometeor.*, **5**, 267–285, https://doi.org/10.1175/1525-7541(2004)005<0267:SOTCHC>2.0.CO;2.

Vörösmarty, C. J., P. Green, J. Salisbury, and R. B. Lammers, 2000: Global water resources: Vulnerability from climate change and population growth. *Science*, **289**, 284–288, https://doi.org/10.1126/science.289.5477.284.

Wang, G., J. Xia, and J. Chen, 2009: Quantification of effects of climate variations and human activities on runoff by a monthly water balance model: A case study of the Chaobai River basin in northern China. *Water Resour. Res.*, **45**, W00A11, https://doi.org/10.1029/2007WR006768.

Wang, H., Z. Yang, Y. Saito, J. P. Liu, and X. Sun, 2006: Interannual and seasonal variation of the Huanghe (Yellow River) water discharge over the past 50 years: Connections to impacts from ENSO events and dams. *Global Planet. Change*, **50**, 212–225, https://doi.org/10.1016/j.gloplacha.2006.01.005.

Wang, W., Q. Shao, T. Yang, S. Peng, W. Xing, F. Sun, and Y. Luo, 2013: Quantitative assessment of the impact of climate variability and human activities on runoff changes: A case study in four catchments of the Haihe River basin, China. *Hydrol. Processes*, **27**, 1158–1174, https://doi.org/10.1002/hyp.9299.

Xiong, W., I. Holman, E. Lin, D. Conway, J. Jiang, Y. Xu, and Y. Li, 2010: Climate change, water availability and future cereal production in China. *Agric. Ecosyst. Environ.*, **135**, 58–69, https://doi.org/10.1016/j.agee.2009.08.015.

Xu, K., J. D. Milliman, and H. Xu, 2010: Temporal trend of precipitation and runoff in major Chinese Rivers since 1951. *Global Planet. Change*, **73**, 219–232, https://doi.org/10.1016/j.gloplacha.2010.07.002.

Xu, X., D. Yang, H. Yang, and H. Lei, 2014: Attribution analysis based on the Budyko hypothesis for detecting the dominant cause of runoff decline in Haihe basin. *J. Hydrol.*, **510**, 530–540, https://doi.org/10.1016/j.jhydrol.2013.12.052.

Yang, H., and Coauthors, 2015: Multicriteria evaluation of discharge simulation in Dynamic Global Vegetation Models. *J. Geophys. Res. Atmos.*, **120**, 7488–7505, https://doi.org/10.1002/2015JD023129.

Yang, S. L., K. H. Xu, J. D. Milliman, H. F. Yang, and C. S. Wu, 2015: Decline of Yangtze River water and sediment discharge: Impact from natural and anthropogenic changes. *Sci. Rep.*, **5**, 12581, https://doi.org/10.1038/srep12581.

Yang, T., X. Chen, C. Y. Xu, and Z. C. Zhang, 2009: Spatio-temporal changes of hydrological processes and underlying driving forces in Guizhou region, Southwest China. *Stochastic Environ. Res. Risk. Assess.*, **23**, 1071–1081, https://doi.org/10.1007/s00477-008-0278-7.

Ye, X., Q. Zhang, J. Liu, X. Li, and C. Xu, 2013: Distinguishing the relative impacts of climate change and human activities on variation of streamflow in the Poyang Lake catchment, China. *J. Hydrol.*, **494**, 83–95, https://doi.org/10.1016/j.jhydrol.2013.04.036.

Ye, Y., X. Fang, Y. Ren, X. Zhang, and L. Chen, 2009: Cropland cover change in Northeast China during the past 300 years. *Sci. China*, **52D**, 1172–1182, https://doi.org/10.1007/s11430-009-0118-8.

Yin, J., F. He, Y. J. Xiong, and G. Y. Qiu, 2017: Effects of land use/land cover and climate changes on surface runoff in a semi-humid and semi-arid transition zone in northwest China. *Hydrol. Earth Syst. Sci.*, **21**, 183–196, https://doi.org/10.5194/hess-21-183-2017.

Yin, X., P. C. Struik, P. Romero, J. Harbinson, J. B. Evers, P. E. L. Van Der Putten, and J. Vos, 2009: Using combined measurements of gas exchange and chlorophyll fluorescence to estimate parameters of a biochemical C3 photosynthesis model: A critical appraisal and a new integrated approach applied to leaves in a wheat (Triticum aestivum) canopy. *Plant Cell Environ.*, **32**, 448–464, https://doi.org/10.1111/j.1365-3040.2009.01934.x.

Zhang, C., B. Zhang, W. Li, and M. Liu, 2014: Response of streamflow to climate change and human activity in Xitiaoxi

river basin in China. *Hydrol. Processes*, **28**, 43–50, https://doi.org/10.1002/hyp.9539.

Zhang, L., R. Karthikeyan, Z. Bai, and R. Srinivasan, 2017: Analysis of streamflow responses to climate variability and land use change in the Loess Plateau region of China. *Catena*, **154**, 1–11, https://doi.org/10.1016/j.catena.2017.02.012.

Zhang, Q., C. Xu, S. Becker, and T. Jiang, 2006: Sediment and runoff changes in the Yangtze River basin during past 50 years. *J. Hydrol.*, **331**, 511–523, https://doi.org/10.1016/j.jhydrol.2006.05.036.

——, V. P. Singh, P. Sun, X. Chen, Z. Zhang, and J. Li, 2011: Precipitation and streamflow changes in China: Changing patterns, causes and implications. *J. Hydrol.*, **410**, 204–216, https://doi.org/10.1016/j.jhydrol.2011.09.017.

Zhang, Z., X. Chen, C. Xu, L. Yuan, B. Yong, and S. Yan, 2011: Evaluating the non-stationary relationship between precipitation and streamflow in nine major basins of China during the past 50 years. *J. Hydrol.*, **409**, 81–93, https://doi.org/10.1016/j.jhydrol.2011.07.041.

Zhou, G., and Coauthors, 2010: Forest recovery and river discharge at the regional scale of Guangdong Province, China. *Water Resour. Res.*, **46**, W09503, https://doi.org/10.1029/2009WR008829.

——, and Coauthors, 2015: Global pattern for the effect of climate and land cover on water yield. *Nat. Commun.*, **6**, 5918, https://doi.org/10.1038/ncomms6918.

Zhu, D., and Coauthors, 2015: Improving the dynamics of Northern Hemisphere high-latitude vegetation in the ORCHIDEE ecosystem model. *Geosci. Model Dev.*, **8**, 2263–2283, https://doi.org/10.5194/gmd-8-2263-2015.

Zhu, Z., and Coauthors, 2016: Greening of the Earth and its drivers. *Nat. Climate Change*, **6**, 791–795, https://doi.org/10.1038/nclimate3004.